Journal of Applied Fluid Mechanics, Vol. 16, No. 4, pp. 717-723, 2023.
Available online at www.jafmonline.net, ISSN 1735-3572, EISSN 1735-3645.
https://doi.org/10.47176/jafm.16.04.1581

Influence of Surface Curvature on Coanda Effect for Vertical Jet Impacting Horizontal Cylinder

M. Nausin[1], M. Seerwani[1], M. M. Alam[2,†]

[1] *Shen Wai International School (SWIS), 29 Baishi Third Road, Nanshan, Shenzhen, China*
[2] *Harbin Institute of Technology (Shenzhen), Shenzhen 518055, China*

†*Corresponding Author Email: alamm28@yahoo.com; alam@hit.edu.cn*

(Received September 22, 2022; accepted November 24, 2022)

ABSTRACT

The Coanda effect is a tendency of flowing fluid to follow the solid surface rather than to separate under the inertial effect. This paper presents the effects of surface curvature on the Coanda angle and jet deflection for a vertical jet impacting a horizontal cylinder (of diameter D) with Froude numbers Fr = 4.74 and 6.33. The penetration depth h of the cylinder in the jet is varied from h/D = 0.01–0.4 while the jet-to-cylinder diameter ratio d/D is varied from 0.11 to 2.0. For Fr = 4.74, the round jet impacting the cylinder evolves into a planar jet for $d/D \leq 0.40$ where the jet deflection is positive, dictated by the Coanda effect. The deflection of the jet is negative for d/D = 0.60 and 0.83 where the bouncing (inertial) effect overwhelms the Coanda effect. Fr = 4.74, the jet deflects in the positive direction, regardless of d/D. With increasing h/D or decreasing d/D, both deflection and Coanda angles monotonically increase. An intermittent switch of the jet from one side of the cylinder to the other is observed for certain curvature of the cylinder, ascribed to the competition between bouncing and Coanda effects.

Keywords: Coanda effect; Jet; Cylinder; Bouncing effect; Curvature.

NOMENCLATURE

d	jet diameter	Q	flow rate
D	cylinder diameter	θ	Coanda angle or wettability angle
h	penetration depth	α	jet deflection angle
V	jet velocity		

1. INTRODUCTION

The Coanda effect is an interaction between flowing fluid and solid surface whereby the flow undergoes a tendency to follow the surface curvature rather than separation under inertial motion. It is seen to occur in nature, daily life, and engineering. For example, in our daily life, it is quite hard to pour water, Coca-Cola, or juice from one glass to another (Fig. 1a, b). When water, Coca-Cola, or juice is poured from one glass to another, the water, Coca-Cola, or juice does not directly fall from the glass edge but spills over the outer side surface of the glass. When we use a room heater, warm air from the heater follows a nearby wall. The warm air along a window pane renders heat to the window glass and prevents condensation. In engineering, aircraft wings make use of the Coanda effect to generate lift force. So do wind turbine blades. In addition to engineering applications, many examples of the Coanda principle are found in the natural world. For example, Eisner and Aneshansley (1982) reported that Bombardier beetles, when disturbed, eject a defensive fluid (a hot quinine-containing secretion) and rely on the Coanda effect for aiming.

Artificial respiration provides for the overall exchange of gases in the body through pulmonary ventilation, external respiration, and internal respiration (Lubert 2010). Doctors use an endotracheal tube for airway management and as an alternative route for drugs (Fig. 1c). The tube inserted into a patient's trachea allows air to reach the lungs. Jackson (1971) suggested that an endotracheal tube with a self-inflating cuff can be employed advantageously to guide air into the cuff for inflation purposes so that airflow tends to hug and follow the direction of a surface (Fig. 1c). A water flosser, also known as a water pick that shoots water jet to flush food particles and plaque off of teeth (Fig. 1d). The cleaning effectiveness depends on water jet velocity,

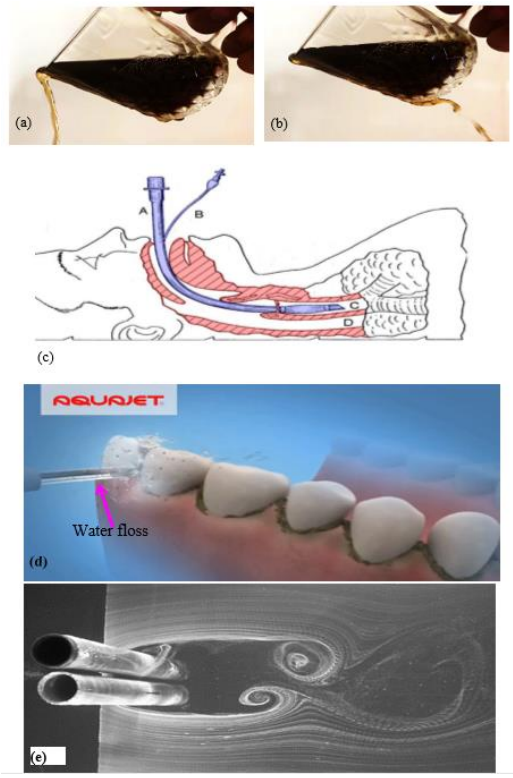

Fig. 1. Coanda effects (a, b) when water Coca-Cola poured slowly from glass; (c) in artificial respiration - A: endotracheal tube, B: cuff inflation tube with pilot balloon, C: trachea, D: esophagus (Lubert 2010); (d) in water-jet flossing; and (e) when gap flow deflected for two side-by-side cylinders (Alam *et al.* 2003).

pulsation and diameter where the jet may undergo Coanda effect or reflection (Jolkovsky and Lyle 2015; Alharib and Farah 2020).

The Coanda effect has also been very successfully employed in storm or lake water filtration where the water often contains dirt, grit, leaves and other debris which can congregate within the conduits, reduce the throughput, and ultimately make the system ineffective (Esmond *et al.* 2004). Using the Coanda effect can separate the water from the debris as the water is susceptible to the Coanda effect but the debris is not.

Romanian aerodynamics pioneer Henri Coanda was the first person to build and fly the Coanda-1910 aircraft in 1910. He failed to make the aircraft off the ground as the aircraft burst into flame during its warmup. It was, however, not a waste as he discovered something unusual that is the Coanda effect.

Skotnicka-Siepsiak (2022) examined the Coanda effect on a flat plate placed in an asymmetrical wall jet issued from a diffuser outlet. The inclination angle of the flat plate was varied from 0° and 90°, and the Coanda effect hysteresis was examined. He observed the Coanda effect hysteresis on flow reattachment, separation bubble, and pressure distribution. It has been demonstrated that for a jet flow, pressure distribution on the fat plate is determined not only by the inclination angle of the plate but also by the direction of its rotation.

Lai and Lu (1996) examined distributions of velocities and turbulence, and the position of jet reattachment on a plate for the plate inclination angles of 0° (flowing over the wall), 15°, 30°, 45°, and 90° (free jet). They measured pressure distribution to pinpoint the position of the jet reattachment to the plate and made flow visualizations to visualize the flow reattachment. They found that an increase in the plate inclination angle decreases the axial velocity and jet core zone while increasing the jet area.

In heat exchangers, the heat exchange between two fluids occurs via solid tubes where one fluid flows over the tube surfaces and the other fluid flows inside the tubes. The tube cooling or heating by the fluid flow over the tubes is the measure of the heat exchange and is determined by the Coanda effect; the larger the attached flow boundary, the greater the heat transfer (Alam *et al.* 2020; Abdelhamid *et al.* 2021). The gap flow between two side-by-side or staggered cylinders undergoes Coanda effects and deflects toward a cylinder (e.g. Ishigai *et al.* 1972; Alam *et al.* 2003; Alam *et al.* 2005; Alam and Zhou 2007), see Fig. 1e. The degree of the deflection angle was found to be dependent on the spacing between the cylinders and the Reynolds number. For a cylinder placed symmetrically in a two-dimensional finite-width jet, Schuh and Person (1964) achieved a 20% enhancement of heat transfer as the Coanda effect causes the jet to adhere to the cylinder.

Jambon-Puillet *et al.* (2019) examined the behaviors of a fluid jet striking a vertical cylinder. They found the jet after striking the cylinder for a spiral rivulet, and its shape depends on the initial speed and geometry of the jet.

The above review indicates that the Coanda effect has implications in various fields. Particular implications of a jet impacting on cylinder like-structures are the gap flow between two cylinders and water-jet flossing. However, there are no fundamental studies on these issues. This investigation aims to understand the Coanda effect on a horizontal cylinder. Particular attention is paid to how surface curvature and jet diameter affect the wettability and deflection of the jet flow (Fig. 2a). From an engineering point of view, understanding the Coanda effect has crucial importance not only for designing food containers but also for better control of jet flows.

2. EXPERIMENTAL DETAILS

The experiment was done with a vertical water jet from a water tap while the cylinder was horizontal, held on a camera tripod stand using a C-clamp, as shown in Figs. 2(b, c). The cylinder was made horizontal using a tubular spirit level (Fig. 2c). The cylinder position was 215 cm away from the exit of the tap. The diameter of the jet at the cylinder position is denoted by d while the cylinder diameter is denoted by D (Fig. 2a).

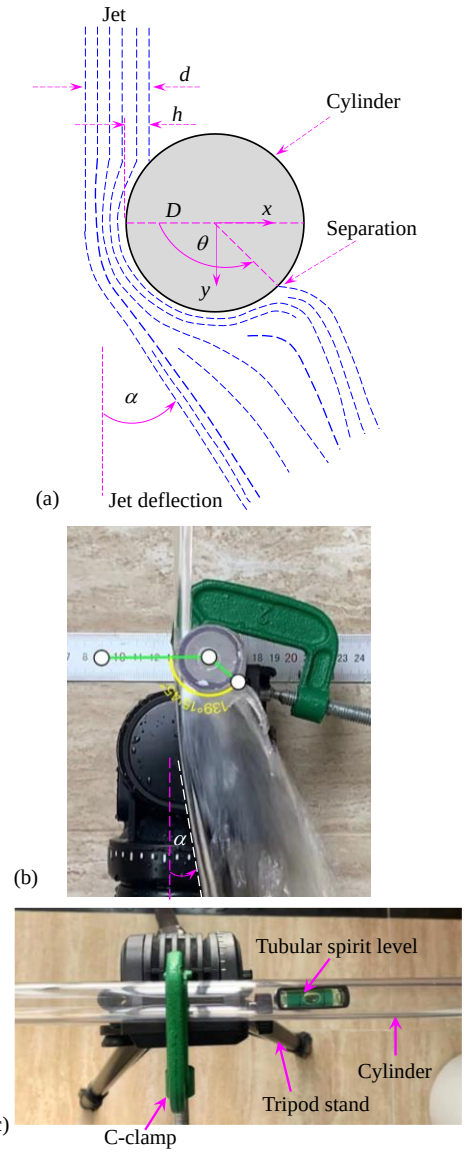

Fig. 2. (a) Sketch showing jet deflection, separation, and definitions of symbols. (b) A corresponding representative snapshot of jet and angle measurement using angle meter app. (c) Photograph of experimental setup.

We changed the cylinder surface curvature by changing the cylinder diameter as D = 5, 10, 15, 18, 25, 30, and 55 mm. The jet diameter was varied by tuning the tap knob. The jet diameter was measured from a snapshot of the jet, which was scaled with a ruler fixed on the wall (Fig. 2b) as well as with the cylinder diameter measured directly by a slide caliper. We chose two values of the jet diameter d = 6 mm and 10 mm. When d is known, the average flow velocity V of the jet at the cylinder position was measured by collecting water (Q litter) in a beaker for 60 seconds as $V = \frac{4(Q/60)\times 10^3}{\pi d^2}$ m/s, where the time was measured using a stopwatch. The jet diameter d = 0.6 and 1.0 cm correspond to the jet velocity V = 1.15 and 1.95 m/s, respectively, yielding Froude number Fr ($=V/\sqrt{gd}$) = 4.74 and 6.23, respectively. The Froude number is a dimensionless number defined as the ratio of the inertia force on a fluid element to the weight of the fluid element. We varied the penetration depth h of the cylinder in the jet as h/D = 0.01, 0.10, 0.25, and 0.4 (Fig. 2a). Here, the Cartesian coordinate (x, y) system is employed, with the origin at the center of the cylinder.

For each combination of d/D and h/D, videos of the flow were recorded for 30 seconds using a camera with 30 frames/second. From each video, 10 snapshots were arbitrarily taken for measuring the wettability angle θ (also called the Coanda angle) and jet deflection angle α (Fig. 2a). We used an app called 'angle meter' in the iPhone app store to measure the angles (Fig. 2b). It is a very convenient tool, having a resolution of 1 second (i.e. 0.00027°), to measure angles in images. The separation point was identified from a zoomed-in view of the snapshot around the jet flow separation. Its azimuthal angle θ was then measured using the angle meter app (Fig. 2b). On the other hand, the jet deflection angle was measured as the angle α of the deflected jet (the white dashed line) with respect to the vertical line (the red dashed line), see Fig. 2b. The average value of α was considered for the 10 snapshots. So was that of θ.

3. RESULTS AND DISCUSSION

The results are presented for two jet diameters and two jet velocities. The jet diameter d = 6 mm, V =1.15

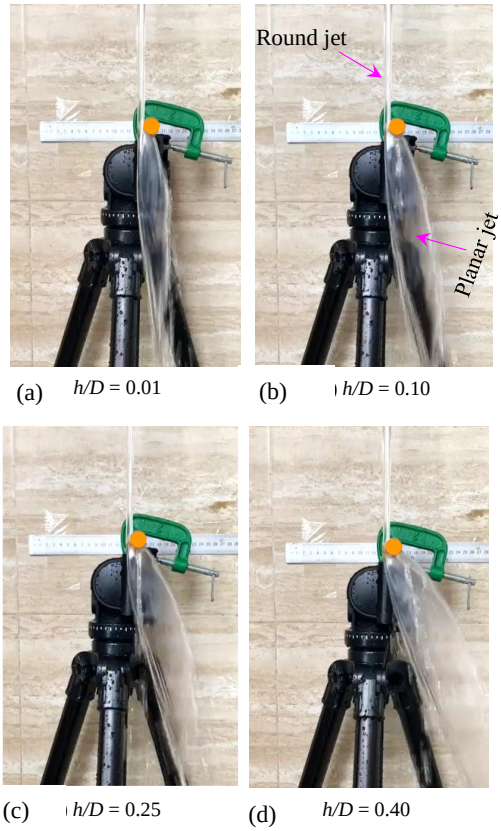

Fig. 3. Snapshots of jet flow for different h/D values at jet-to-cylinder diameter ratio d/D = 0.4 and Froude number Fr = 4.74.

m/s corresponds to Fr = 4.74, while d = 10 mm 1.95 m/s to Fr = 6.23. The former is herein referred to as the small Fr jet and the latter is as the large Fr jet. The penetration depth h of the cylinder in the jet is varied as h/D = 0.01, 0.10, 0.25, and 0.4.

3.1 Small Froude-number Jet

Figure 3 shows snapshots of the flow when h/D is varied as h/D = 0.01, 0.10, 0.25 and 0.40 for d/D = 0.4 (d = 6 mm, D = 15 mm) and Fr = 4.74. As seen in the figure, once hitting the cylinder, the round jet evolves into a planar jet. The planar jet deflects toward the opposite side (i.e. +*ve* α) of the cylinder. Interestingly, the deflection angle α of the jet increases as h/D increases, as does the Coanda angle θ. The Coanda angle is greater than 90° for all h/D values presented. The sheet width firstly widens and then shrinks, reaching a maximum at y/D = 5–10 (depending on h/D) away from the cylinder center. The variation of the jet width is largely due to the variation of the profile of the flow issuing from the separation point on the cylinder.

At a smaller d/D = 0.6, the scenario is different. As shown in Fig. 4, now the jet deflects toward the same side (i.e. -*ve* α) of the cylinder. Again, when h/D is

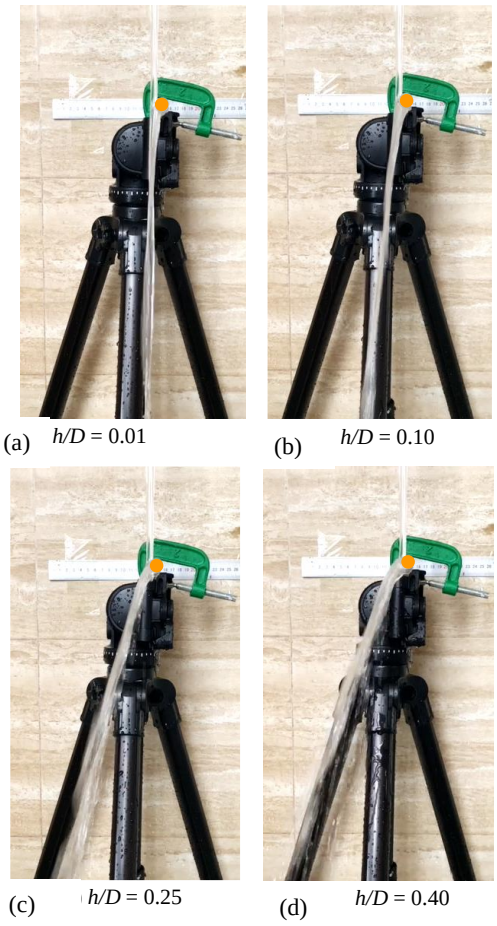

Fig. 4. Snapshots of jet flow for different h/D values at jet-to-cylinder diameter ratio d/D = 0.6 and Froude number Fr = 4.74.

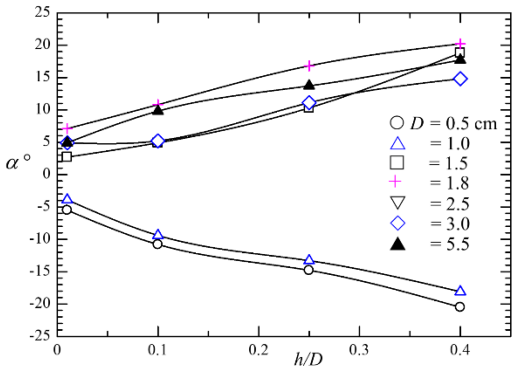

Fig. 5. Dependence of jet deflection angle α on h/D and d/D for Froude number Fr = 4.74 (d = 6 mm, V = 1.15 m/s).

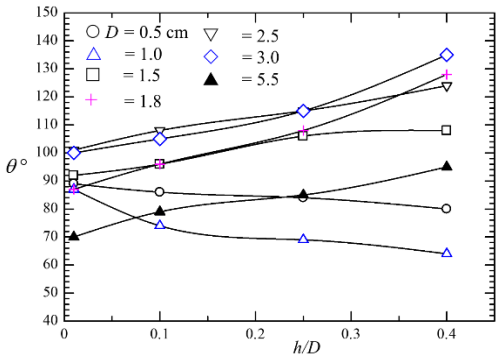

Fig. 6. Dependence of jet deflection angle θ on h/D and d/D for Froude number Fr = 4.74 (d = 6 mm, V = 1.15 m/s).

increased, the jet deflection enhances but the Coanda angle slightly decreases, being less than 90°. For the negative jet deflection, the jet following the cylinder remains more or less round.

The effects of the penetration depth ratio h/D and d/D on the jet deflection angle α for Fr = 4.74 are presented in Fig. 5. Interestingly, the jet deflection angle is highly dependent on both h/D and d/D. The deflection angle is negative for large d/D values (i.e., d/D = 0.60 and 1.2) while positive for small d/D (≤ 0.40) values. This observation suggests that when the cylinder curvature is sufficiently large (i.e. large d/D), the jet bouncing effect (i.e. inertial effect) becomes predominant and causes the negative deflection of the jet. With increasing h/D, the deflection angle monotonically decreases for d/D = 0.60 and 1.2 but increases for $d/D \leq 0.40$.

Figure 6 shows the Coanda angle dependence on h/D and d/D. Again, there are two distinguished trends of the Coanda angle dependence on h/D and d/D, one for d/D = 1.20 and 0.6, where the Coanda angle decreases with h/D and the other for $d/D \leq 0.4$, where the Coanda angle increases. For a given h/D, the dependence of the Coanda angle on d/D is however non-linear. The Coanda angle lies between 64° and 138° in the h/D and d/D ranges examined.

3.2 Large Froude-number Jet

Similarly, the relationship of the jet deflection anglewith *h/D* and *d/D* is presented in Fig. 7 for *Fr* = 6.23. For this *Fr* value, the deflection angle monotonically rises with *h/D* and *d/D*. The rise of the deflection angle with *h/D* is larger for a smaller *d/D*. As such, the increase in the deflection angle with decreasing *d/D* is larger for a larger *h/D*.

Figure 8 depicts the Coanda angle dependence on *h/D* and *d/D*. Now all values of the Coanda angle are larger than 90°, reaching upto 142° for *d/D* = 0.18, *h/D* = 0.4. A larger *h/D* or a smaller *d/D* results in augmentation of the Coanda angle. Again, the Coanda angle increase with decreasing *d/D* is larger at a higher *h/D*.

3.3 Jet instability at small gap

An interesting observation is made when the jet is close to the cylinder with a small gap between them. Although there was a gap (i.e. jet not touching the cylinder), the jet was found to unstable to intermittently touch the cylinder and undergo the Coanda effect. Figure 9(a) shows the jet with a gap of about 1 mm. For the time being, the flow was found to be unstable as it intermittently touches the cylinder, see Fig. 9(b) where the jet flow kisses the

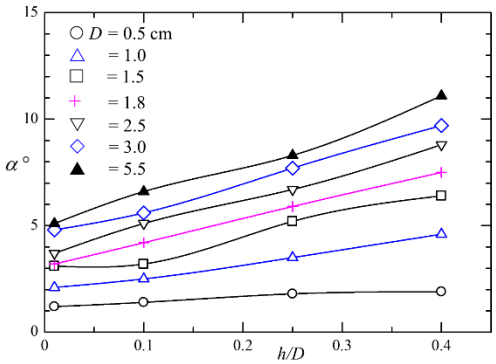

Fig. 7. Dependence of jet deflection angle α on *h/D* and *d/D* for Froude number *Fr* = 6.23 (*d* = 10 mm, *V* = 1.95 m/s).

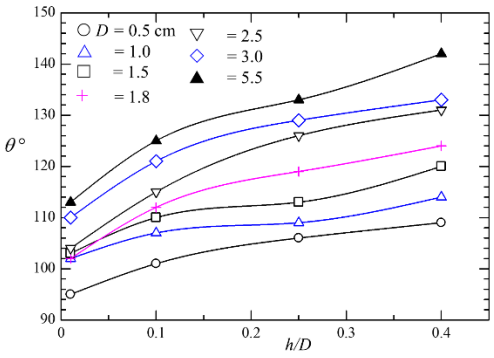

Fig. 8. Dependence of jet deflection angle *θ* on *h/D* and /*D* for Froude number *Fr* = 6.23 (*d* = 10 mm, *V* = 1.95 m/s).

(a) Jet separated by a gap (b) Jet kissing the cylinder

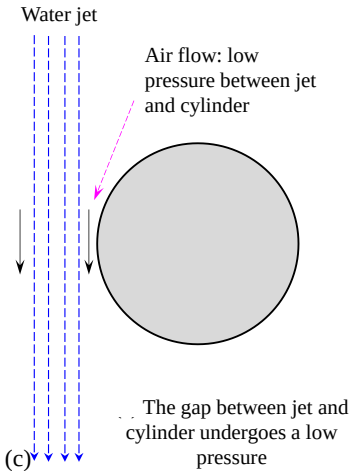

Fig. 9. (a, b) Bistable jet for jet-to-cylinder diameter ratio *d/D* = 0.02 (*d* = 0.6, *D* = 3) and Froude number *Fr* = 4.74. The jet is separated by a gap of 1 mm. (c) Sketch showing low pressure between jet and cylinder because of airflow induced by the viscous action at the interface between jet and air. This low pressure causes the intermittent attachment of the jet albeit there is a gap between the jet and cylinder.

cylinder and generates a very thin planer jet. The main jet does not modify much (see also video 1). Why the jet flow is attracted by the cylinder can be explained with the aid of Fig. 9(c). As sketched in the figure, the water jet causes a downward airflow around it because of viscous action at the interface between the water jet and air. In other words, there is downward airflow in the gap between the jet and cylinder. This airflow results in a low pressure in the gap, which attracts the jet toward the cylinder and gets the jet intermittently touched.

3.4 Jet switch: competition between Coanda and inertia effects

We observed intermittent switches of the jet flow for certain curvatures of the cylinder. In Fig. 5, we showed that, for *d/D* = 0.4 and 0.6, the deflection of the jet was positive and negative, respectively for *Fr*

(a) Negative deflection of jet (b) Positive deflection of jet

Fig. 10. Bistable jet for *d/D* = 0.33 (*d* = 0.5, *D* = 1.5), *h/D* = 0.4 and Fr = 4.37. The jet intermittently switches from (a) the left side to (b) the right side and vice versa.

= 4.74. On the other hand, when *Fr* was increased to 6.23, there were only positive deflections for both *d/D* = 0.4 and 0.6. Interestingly, when *Fr* was slightly decreased to 4.37 for *d/D* = 0.4, we found an intermittent switch of the jet from positive to negative and vice versa (Fig. 10a, b). See also video 2 attached as supplementary material. The intermitted switch may be the consequence of the competition between the inertial (bouncing) and Coanda effects. When the inertial effect overwhelms the Coanda effect, the jet switches from its positive side to negative. An opposite switch prevails when the Coanda effect overwhelms the inertial effect.

5. CONCLUSIONS

In this paper, we aim to experimentally investigate the surface curvature and jet diameter effect on the Coanda angle and jet deflection when a vertical jet impacts a horizontal cylinder. The cylinder surface curvature is changed by changing the cylinder diameter as *D* = 5, 10, 15, 18, 25, 30, and 55 mm while the jet diameter is *d* = 6 and 10 mm corresponding to Froude number *Fr* = 4.74 and 6.23, respectively. We varied the penetration depth *h* of the cylinder in the jet as *h/D* = 0.01, 0.10, 0.25, and 0.4. The investigation leads to the following conclusions.

In the case of the small Froude-number jet, the round jet impacting the cylinder turns into a planar when the jet deflection is positive but remains round when the jet deflection is negative. Positive deflection takes place when the jet-to-cylinder diameter ratio is sufficiently small (i.e. $d/D \leq 0.4$) while negative deflection occurs for the large jet-to-cylinder diameter ratio (i.e. *d/D* = 0.6 and 1.2). While the jet bouncing effect is responsible for the negative deflection, the Coanda effect results in the positive deflection. When *h/D* is increased, both deflection and Coanda angles of the following jet increase for the positive deflection. The scenario is the opposite for the negatively deflected jet.

In the case of the large Froude-number jet, the following jet, regardless of *d/D*, deflects in the positive direction, being planar. The deflection and Coanda angles monotonically increase when *h/D* is increased or *d/D* is decreased. The increase of the angles with increasing *h/D* is larger for a smaller *d/D* while that with decreasing *d/D* is larger for a larger *h/D*. The Coanda angle becomes larger than 90°, being as large as 143° for *d/D* = 0.18, *h/D* = 0.4.

When the jet and cylinder are separated by a small gap, the jet intermittently touches the cylinder and experiences the Coanda effect. A low pressure generated in the gap, due to a downward airflow induced by the viscous action, attracts the jet toward the cylinder and gets the jet intermittently touched.

The jet flow is found to intermittently switch from one side of the cylinder to the other for certain curvature of the cylinder, which is ascribed to the competition between bouncing and Coanda effects.

REFERENCES

Abdelhamid, T., M. M. Alam and M. Islam (2021). Heat transfer and flow around cylinder: Effect of corner radius and Reynolds number. *International Journal of Heat and Mass Transfer* 171, 121105.

Alam, M. M., T. Abdelhamid and A. Sohankar (2020). Effect of cylinder corner radius and attack angle on heat transfer and flow topology. *International Journal of Mechanical Sciences* 179, 105566.

Alam, M. M., H. Sakamoto and Y. Zhou (2005). Determination of flow configurations and fluid forces acting on two staggered circular cylinders of equal diameter in cross-flow. *Journal of Fluids and Structures* 21, 363-394.

Alam, M. M. and Y. Zhou (2007). Flow around two side-by-side closely spaced circular cylinders. *Journal of Fluids and Structures* 23, 799-805.

Alam, M. M., M. Moriya and H. Sakamoto (2003). Aerodynamic characteristics of two side-by-side circular cylinders and application of wavelet analysis on the switching phenomenon. *Journal of Fluids and Structures* 18, 325-346.

Alharib, M. and R. Farah (2020). Effect of water-jet flossing on surface roughness and color stability of dental resin-based composites. *Journal Clinical and Experimental Dentistry* 12(2), 169-177.

Eisner, T. and D. J. Aneshansley (1982). Spray aiming in bombardier beetles: jet deflection by the coanda effect. *Science* 215(4528), 83-85.

Esmond, S. E., L. Quinn and R. K. Weir (2004). Rain and storm water filtration systems (U.S. Patent 6705049).

Ishigai, S., E. Nishikawa, E. Nishimura and K. Cho (1972). Experimental study of structure of gas flow in tube banks axes normal to flow. *Bulletin of the Japan Society of Mechanical Engineers* 15, 949-956.

Jackson, R. R. (1971). Self-Inflating Endotracheal Tube (U. S. Patent 3707151).

Jambon-Puillet, E., W. Bouwhuis, J. H. Snoeijer and D. Bonn (2019). Liquid helix: how capillarity jets adhere to vertical cylinders. *Physical Review Letters* 122, 184501.

Jolkovsky, D. L. and D. M. Lyle (2015). Safety of a water flosser: a literature review. *Compendium of Continuing Education in Dentistry* 36(2), 146-155.

Lai, J. C. S. and D. Lu (1996). Effect of wall inclination on the mean flow and turbulence characteristics in a two-dimensional wall jet. *International Journal of Heat Fluid Flow* 17(4), 377-385.

Lubert, C. (2010, November). On some recent applications of the coanda effect to acoustics. *In Proceedings of Meetings on Acoustics 160ASA*. Acoustical Society of America.

Schuh, H. and B. Person (1964). Heat transfer on circular cylinders exposed to free jet flow. *International Journal of Heat and Mass Transfer* 7, 1257.

Skotnicka-Siepsiak, A. (2022). Pressure distribution on a fat plate in the context of the phenomenon of the Coanda effect hysteresis. *Scientific Reports* 12, 12687.